

Distribution of Natural Radionuclides, Rare Earth Elements, Metals and Metalloids in a Phosphogypsum Stockpile

Maria Jose Madruga^{1,2}, Maria Isabel Prudencio¹, Jose Alberto Gil Corisco^{1,2*}, Jan Mihalik¹, Rosa Marques¹, Marta Santos^{1,2}, Mario Reis^{1,2}, Isabel Paiva^{1,2}, and Maria Isabel Dias¹

¹Center for Nuclear Sciences and Technologies, Department of Nuclear Sciences and Engineering, Instituto Superior Técnico (IST), University of Lisbon (UL), National Road 10, (km 139.7), 2695-066 Bobadela-LRS, Portugal

²Laboratory of Radiological Protection and Safety, IST, UL, National Road 10, (km 139.7), 2695-066 Bobadela-LRS, Portugal

*Corresponding author: Jose Alberto Gil Corisco, Instituto Superior Técnico (IST), University of Lisbon (UL), National Road 10, (km 139.7), 2695-066 Bobadela-LRS, Portugal, Tel: +351 219946269; E-mail: corisco@ctn.tecnico.ulisboa.pt

Received date: January 16, 2019; Accepted date: March 07, 2019; Published date: March 14, 2019

Copyright: © 2019 Madruga MJ, et al. This is an open access article distributed under the terms of the Creative Commons Attribution License, which permits unrestricted use, distribution and reproduction in any medium, provided the original author and source are credited.

Abstract

A first detailed study of phosphogypsum (PG) from a stockpile in Barreiro (Portugal) was performed aiming for a better characterization of this industrial waste deposit, considering its enhanced content in natural radionuclides and toxic metals, making it a potential contamination source to the Tejo estuary. Whole samples and aggregates of these wastes resulting from phosphate industries were analysed by neutron activation, gamma-spectrometry, X-ray diffraction and scanning electron microscopy. This work clearly shows that a significant chemical heterogeneity in the PG occurs due to the existence of aggregates with different compositions randomly distributed. Among these aggregates, the dark grey ones have high concentrations of Sc, Cr, Zn, Ga, Ba, REE, Ta, W, Th and U and the highest concentrations of ²²⁶Ra and ²¹⁰Pb. The separation of these dark aggregates prior to any application of the PG would lead to a safer reuse of these wastes. The chemical patterns, including the REE distribution with a significant negative Ce anomaly, found in PG, are certainly related with the geochemical signatures of the phosphate rocks used as raw material. This PG stockpile may play a significant role as a radioactive source in the Tejo estuarine environment.

Keywords: Gamma spectrometry; Instrumental Neutron Activation Analysis (INNA); Phosphogypsum; Radioactivity; Radionuclides; Rare earth elements; Trace elements; Technologically Enhanced Naturally Occurring Radioactive Materials (TENORM)

Introduction

The environmental impact of massive amounts of phosphogypsum (PG) produced as a waste from the phosphate industry is a worldwide concern due to its content in toxic elements and natural radionuclides. The application of PG, for instance as raw material in building and soil enrichment stuff, or the alternative decision of letting the PG stockpiles remain in place with some further reasonable remediation, demands a characterization of its properties. The PG, the insoluble by-product resulting from the sulfuric acid attack (wet chemical treatment) of the phosphate rock to produce phosphoric acid, has associated high activities of natural radionuclides from U and Th series [1,2] and is designated as a TENORM. This by-product is usually deposited in dumps and stacks of very large volume and surface representing a great danger to the environment [3].

During the phosphoric acid production, the radioactive equilibrium between the ²³⁸U and its daughters (²²⁶Ra, ²¹⁰Pb) is broken and each radionuclide is distributed differently depending on its solubility. Most of the radium is transferred to the PG and the major amounts of the uranium partition into the phosphoric acid [4,5]. PG stockpiles contain two main types of mineral phases: a) the original materials which were not modified during acidification and b) minerals formed during acidification. The majority of minerals (up to 95%) belong to the second group, which is formed mainly of bassanite and gypsum [3,6]. High contents of sodium fluorosilicate have also been reported [7]. In addition, other minerals are usually present such as anhydrite,

calcite, quartz, mica, phyllosilicates and phosphate-bearing phases [6,8]. High concentrations of Rare Earth Elements (REE) may be also expected, since some phosphate minerals are usually rich in these elements [9]. Site-specific contamination levels of REE and natural radionuclides in an estuarine ecosystem related to phosphate industry were reported by [10].

The Portuguese phosphate plant located in the vicinity of the Tejo river estuary, started its activity in the years 1950 and has produced phosphoric acid and dumped tons of PG in sludge ponds [11]. From 1979 to 1989, the decanted PG was stockpiled (approximately 6 m thick) over a selected area of the close shore line, on the north-eastern extreme of the Barreiro peninsula [12]. This decommissioned industry was dealing with a specific raw material—North African phosphate rock—with a high content of trace metals and natural radioactive elements mainly from the ²³⁸U decay series [11]. By the end of the industrial activity, about 1.1×10⁶ m³ of PG covered an area of 1.0×10⁵ m² [12]. As a consequence of land use for the construction of a wastewater treatment plant launched in 2007, a considerable amount of PG was removed and re-settled over the remaining stockpile, covering nowadays an area of about 5.5×10⁴ m², disturbing the former vertical profile distribution.

High concentrations of ²²⁶Ra were found in suspended and dissolved forms in the Tejo estuary and attributed to weathering and dissolution processes of the PG stockpile [13]. An assessment of the main radioactive sources (natural and artificial radionuclides) existing

around the Tejo estuary showed an enhancement of ^{210}Pb and ^{210}Po activity concentrations in some locations in the estuary, both in the bottom sediments and in the water column, which were attributed to the spreading of particles from the PG stockpile to the evolving offshore area by the action of wind and runoff [14]. Moreover it has been demonstrated that leaching this PG with 1 mol L^{-1} HCl resulted in a 2.2% extraction efficiency of ^{226}Ra , pointing to a potential radioactive source in the Tejo estuarine environment [15]. Bioavailability of ^{226}Ra and ^{210}Pb was evidenced by particularly high concentrations in the mosses covering the stockpile and, in a lesser extent, herbaceous plants [15]. Thus, one of the main concerns of the PG stockpile in Tejo estuarine margin is on the transport of radionuclides and other toxic elements into water bodies and surrounding soil, as well as the potential hazard of bioaccumulation. In this work, a first detailed evaluation of the distribution of chemical elements including radionuclides in the upper part of this PG stockpile (Portugal) is performed by means of neutron activation, gamma-spectrometry, X-ray diffraction and scanning electron microscopy techniques.

The specific objectives are: (1) the assessment of the chemical, mineralogical and radiometric composition of the PG-whole samples and aggregates; and (2) to evaluate the degree of heterogeneity of the Barreiro PG stockpile (Tejo estuary, Portugal).

Materials and Methods

Sample preparation

Three spots from Barreiro PG stockpile were selected randomly for this work (#1-#3) (Figure 1). The more exposed part of the stockpile (top layer 20 cm depth) was studied and composite samples were collected within square areas of 1 m^2 for each spot. In addition, one soil sample collected close to the PG stockpile, corresponding to a soil developed on estuarine sediment (#4), was also studied.

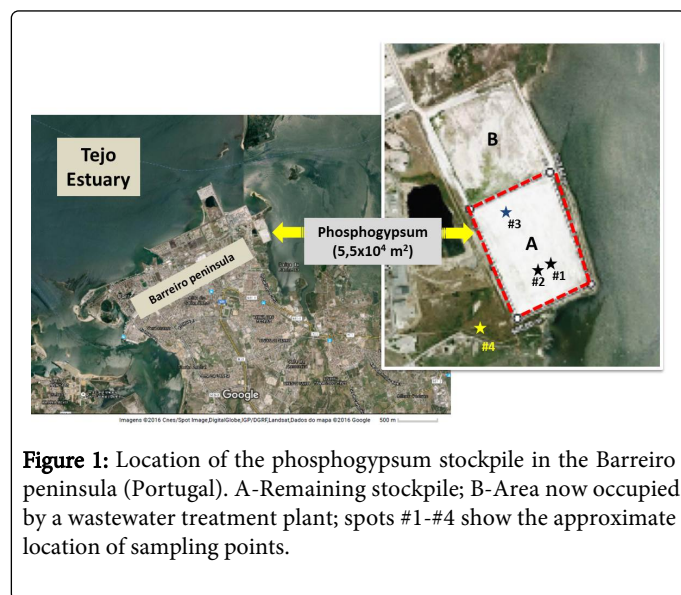


Figure 1: Location of the phosphogypsum stockpile in the Barreiro peninsula (Portugal). A-Remaining stockpile; B-Area now occupied by a wastewater treatment plant; spots #1-#4 show the approximate location of sampling points.

The PG and soil samples were sieved through a 1 mm nylon mesh sieve (whole sample), dried at 50°C and ground in agate mortars for chemical and mineralogical analysis, and in porcelain for radiometry. Aggregates (non-consolidated) with different color and texture were found in the PG stockpile: dark grey, white, and layered grey

aggregates most probably corresponding to remobilization from a fragment of the bottom layered material of the decantation pond. For a more detailed study, aggregates from the PG (#1) sample were selected, separated and prepared for analysis (Figure 2).

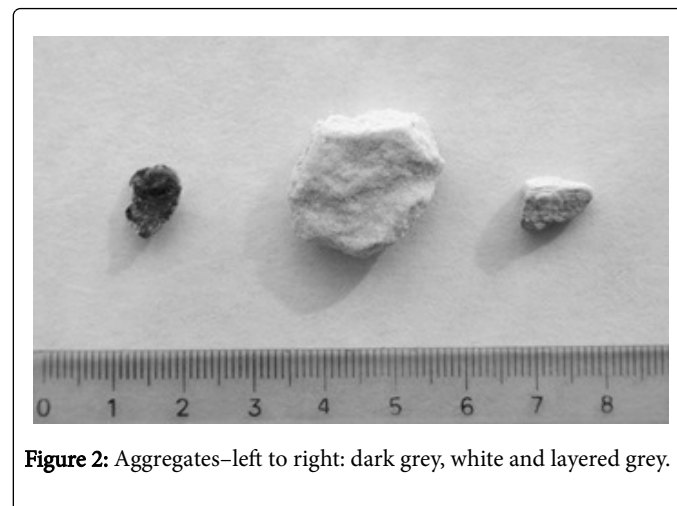


Figure 2: Aggregates—left to right: dark grey, white and layered grey.

Mineralogical and chemical analysis

The mineralogical composition was obtained by X-Ray Diffraction (XRD) of randomly oriented specimens using a Philips diffractometer, Pro Analytical, with Cu K α radiation at 45 kV and 40 mA, a step size of $1^\circ 2\theta/\text{min}$ from 3° to $70^\circ 2\theta$. Mineral identification was done according to the principles stated in specialized literature [16,17].

The chemical analysis was performed by INAA to obtain the concentrations of 31 chemical elements (Na, K, Ca, Mn, Fe, Sc, Cr, Co, Zn, Ga, As, Br, Rb, Zr, Sb, Cs, Ba, La, Ce, Nd, Sm, Eu, Tb, Dy, Yb, Lu, Hf, Ta, W, Th and U). Two multi-element reference materials were used, namely soils GSS-4 and GSS-5 from the Institute of Geophysical and Geochemical Prospecting (IGGE). Reference values were taken from tabulated data [18]. The samples and standards were prepared for analysis by weighing 200-300 mg of powder into cleaned high-density polyethylene vials. Two aliquots of each standard were used for internal calibration, and standard checks were performed (QA/QC). Short (90 s) and long irradiations (6 h) were carried out in the core grid of the Portuguese Research Reactor (CTN/IST, Bobadela) at a thermal flux of $3.96 \times 10^{12} \text{ n cm}^{-2} \text{ s}^{-1}$, $\phi_{\text{thi}}/\phi_{\text{epi}}=96.8$, and $\phi_{\text{th}}/\phi_{\text{fast}}=29.8$ [19]. A Gamma Analyst Integrated Spectrometer (Canberra), with a broad energy Ge (BEGe) detector (model BE3830) connected to a DSA2000 (Canberra) multichannel analyzer, was used. This system has a FWHM of 450 eV at 5.9 keV, 750 eV at 60 keV, and 2100 eV at 122 keV. Corrections for the spectral interference from U fission products in the determination of Ba, REE and Zr were made. Details of the analytical method may be found elsewhere in specialized literature [20-23]. Relative precision and accuracy are, in general, to within 5%, and occasionally within 10%.

The particle chemical analyses and the morphological characterization were performed using a FEG-SEM (field emission guns-scanning electron microscope) JEOL JSM-7001F, with acquisition of digital images in both secondary (SEI) and backscattered (BEI) electron images modes, operated at 20 keV. This device was coupled to an EDX microprobe, and the chemical analysis was performed using the Oxford INCA 250 software.

Radiometric analysis by gamma spectrometry

After homogenization, the aliquots of whole samples were packed in sealed plastic containers of 170 mL and stored for one month to reach the radioactive equilibrium needed to accurately quantify the activity of ²²⁶Ra and ²²⁸Ra using their progenies. A 50% relative efficiency broad energy HPGe detector (Canberra BEGe model BE5030), with an active volume of 150 cm³ and a carbon window was used for the gamma spectrometry measurements. The detector was shielded from the environmental radioactive background by a lead shield with copper and tin lining. Standard nuclear electronics was used and the software GenieTM 2000 [24] was employed for the data acquisition and spectral analysis. The detection efficiency was determined using NIST-traceable multi-gamma radioactive standards (Eckert & Ziegler Isotope Products) with an energy range from 46.5 keV to 1836 keV and customized in a water-equivalent epoxy resin matrix (density of 1.15 g/cm³) to exactly reproduce the geometries of the samples. GESPECOR software [25] was used to correct for matrix (self-attenuation) and coincidence summing effects, as well as to calculate the efficiency transfer factors from the calibration geometry to the measurement geometry (whenever needed). The acquisition time was set to 24 hours and the photopeaks used for the activity determination were: 46.5 keV for ²¹⁰Pb; 295.2 keV, 351.9 keV and 609.3 keV for ²²⁶Ra; 338.3 keV, 911.2 keV and 968.9 keV for ²²⁸Ra; 143.8 keV for ²³⁵U. The ²³⁸U activity was calculated through the ²³⁴Th photopeaks (63.3 keV and 92.4 keV) by assuming secular equilibrium. The stability of the system (activity, FWHM, centroid) was checked at least once a week with a ¹⁵²Eu certified point source. External QC was assured through the participation in intercomparison exercises organized by international organizations [26]. This technique is accredited according to the ISO/IEC 17025:2005 standards.

Results and Discussion

Mineralogical and chemical composition

The mineralogical composition obtained by XRD showed that gypsum dominates in all the PG samples; small and variable amounts of brushite and bassanite as well as traces of quartz, K-feldspars and Ti oxides were found. All aggregates from PG (#1) are gypsum rich. In the dark grey aggregates high amounts of bassanite and traces of Ti oxide occur; in the white aggregate a significant amount of brushite was found; in the layered grey aggregates bassanite was also detected. The occurrence of brushite could be expected in PG due to the mixing properties of the Ca(SO₄,HPO₄).2H₂O solid solution [27]. The soil sample (#4) is mainly composed of quartz and K-feldspars; small amounts of phyllosilicates and traces of gypsum and brushite were also detected, pointing to some contribution from the PG stockpile in close vicinity.

The chemical contents of major, minor and trace elements obtained by INAA of PG and soil whole samples are given in Table 1. The mean values for PG whole samples and the variation coefficients (c) are also shown. Significant variations were found: (i) c<10% for Ca, Cr, Ce, W; (ii) c=10-25% for Na, Ga, Zr, Ba, La, Nd, Sm, Eu, Tb, Dy, Yb, Lu, Ta, Th; (iii) c=25-50% for Fe, Sc, Mn, Co, Rb, Cs, Hf, U; and (iv) c>50% for K, Zn, As, Br, Sb. These variations can be explained by heterogeneity of the PG materials, and the existence of different proportions of aggregates in the PG samples. In fact, the three types of aggregates analyzed showed rather different chemical composition (Table 2); the dark grey ones have high amounts of the majority of the chemical elements, particularly Sc, Cr, Zn, Ga, Ba, REE, Ta, W, Th and U.

Indeed, while the white aggregates were mostly formed of the minerals created during the acidification, the dark grey aggregates probably contained mineral phases inherited from the parent rock which were resistant to the effect of acids, and show high concentrations of metals. The presence of undissolved rock particles coated by gypsum was already reported for phosphogypsum samples from United States [28,29]. Although brushite and gypsum were detected in the studied soil, its chemical composition is typical of a soil developed in estuarine sediment [30-32].

Contents	PG					Soil (#4)	Mean PG/Soil
	(#1)	(#2)	(#3)	Mean	C%		
Na ₂ O*	0.0462	0.0581	0.0361	0.047	19.2	0.0641	0.73
K ₂ O*	0.0648	0.0962	0.0135	0.058	58.6	0.538	0.11
CaO*	37.3	35.6	35.7	36.2	2.2	1.87	19
Fe ₂ O ₃ T*	0.0614	0.12	0.0565	0.08	36.4	0.902	0.089
Sc	0.578	0.658	0.311	0.52	28.8	1.96	0.27
Cr	10	11.8	11.2	11	6.8	14.8	0.74
Mn	2.82	8.67	4.67	5.39	45.3	35.7	0.15
Co	0.0769	0.154	0.103	0.11	28.8	1.43	0.077
Zn	6.18	17.7	5.99	9.96	55	19.1	0.52
Ga	1.25	1.54	1.15	1.31	12.6	3.57	0.37
As	0.369	1.12	0.205	0.56	70.5	5.91	0.095
Br	0.676	2.35	0.275	1.1	81.7	1.23	0.89
Rb	2.42	4.42	1.98	2.94	36.1	29.9	0.098
Zr	36.8	25.2	32.8	31.6	15.2	32.1	0.98
Sb	0.157	0.546	0.141	0.28	66.6	0.648	0.43
Cs	0.111	0.22	0.34	0.22	41.8	2.15	0.1
Ba	46.9	56	33.6	45.48	20.3	40.3	1.1
La	67.7	74.5	54.1	65.4	13	9.97	6.6
Ce	28.6	29.5	29	29	1.3	19.3	1.5
Nd	46	50.4	34.3	43.6	15.6	10.3	4.2
Sm	9.96	11	7.91	9.62	13.3	1.58	6.1
Eu	2.42	2.69	1.75	2.29	17.3	0.352	6.5
Tb	1.85	2.1	1.27	1.74	20	0.201	8.7
Dy	13.2	15.4	9.28	12.6	20	1.3	9.7
Yb	6.95	7.68	4.6	6.41	20.5	0.685	9.4
Lu	1.15	1.18	0.694	1.01	22.1	0.115	8.8
Hf	0.436	0.241	0.758	0.48	44.6	1.11	0.43
Ta	0.0525	0.063	0.0714	0.06	12.4	0.244	0.25
W	0.304	0.331	0.266	0.3	8.9	0.332	0.9

Th	1.91	2.01	1.1	1.67	24.4	2.77	0.6
U	11.3	13.7	5.87	10.3	31.8	1.65	6.2

Table 1: Chemical contents of the PG and soil whole samples from Barreiro (Portugal) obtained by INAA (major elements* are expressed in % oxide and trace elements in mg kg⁻¹; c % expresses a coefficient of variation).

Contents	Dark grey	White	Layered grey
Na ₂ O*	0.0685	0.0232	0.0303
K ₂ O*	0.0439	0.0175	0.0187
CaO*	39	37.3	38.5
Fe ₂ O ₃ T*	0.0968	0.0192	0.0244
Sc	2.81	0.422	0.957
Cr	56.7	8.5	16.9
Mn	1.19	2.15	0.829
Co	0.0834	0.0397	0.0396
Zn	60.7	6.69	13.8
Ga	3.73	1.53	1.66
As	0.397	0.213	0.242
Br	0.664	0.296	0.3
Rb	3.78	1.9	2.06
Zr	n.d.	92.8	28.3
Sb	0.285	0.118	0.109
Cs	0.187	0.0852	0.0953
Ba	257	29.9	64.7
La	157	65.8	68.4
Ce	59.4	23.6	30.6
Nd	86.5	44.1	46.6
Sm	19.1	9.85	9.69
Eu	4.58	2.36	2.5
Tb	3.85	1.89	2.07
Dy	28.3	13.2	13.7
Yb	21.9	6.56	8.61
Lu	3.99	0.962	1.49
Hf	0.25	1.87	0.123
Ta	0.145	0.058	0.0845
W	0.698	0.313	0.327
Th	7.51	1.13	2.62
U	42.4	7.15	15.5

Table 2: Chemical contents of the aggregates from PG (#1) sample from Barreiro stockpile (Portugal) obtained by INAA (major elements* are expressed in % oxide and trace elements in mg kg⁻¹).

The REE patterns of the PG and soil whole samples relative to chondrites [33-35] are shown in Figure 3. The PG samples have higher contents of REE but a lower fractionation between light REE (LREE) and heavy REE (HREE) ((La/Yb)_C=9.7-11.8), when compared with the soil sample ((La/Yb)_C=14.5). Significant negative Ce anomalies ((Ce/Ce*)=0.20-0.27) occur in PG samples, which is certainly inherited from the phosphate rock (the raw material of the phosphoric acid production). The concentrations of REE obtained in the PG whole samples are lower when compared with data from other PG stockpiles [36,37]. The REE pattern of the soil sample is typical of estuarine sediments with a negative Eu anomaly. The higher concentration of REE in PG corresponds well with several reported results in a literature review [9]: the highest concentrations are reached by LREE, although, the concentration of Nd is higher than of Ce. When soil is not rich on organic matter or iron minerals, topsoil is usually depleted of REE. It occurs because weathering of topsoil and solubility of phosphate minerals. REE are consequently accumulated in lower horizons [38,39].

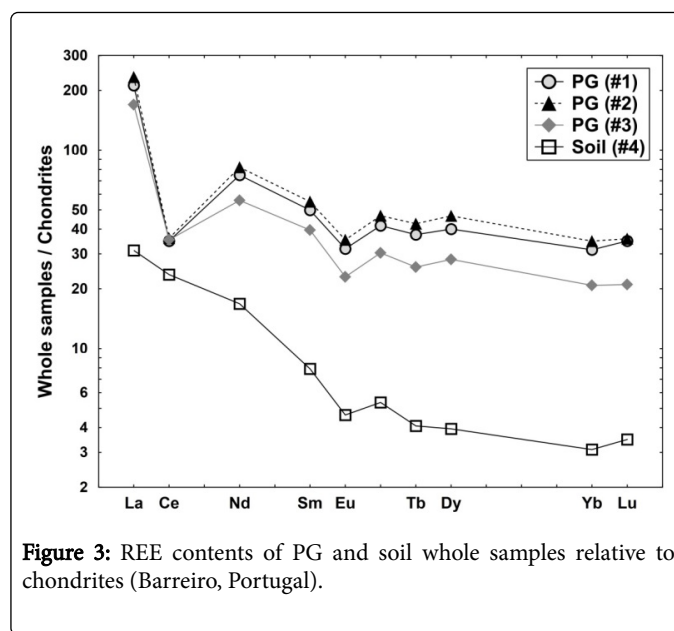


Figure 3: REE contents of PG and soil whole samples relative to chondrites (Barreiro, Portugal).

The chemical content distribution in the aggregates relative to the respective whole sample (PG #1) (Figure 4) shows that: (i) in the dark grey aggregates there is a significant enrichment of the majority of the elements studied, with exception of K, Mn, Zr and Hf; (ii) in the white aggregates only Zr and Hf are present in higher amounts, probably incorporated in zircon minerals; and (iii) the layered grey aggregates have a general intermediate composition, except for the lowest Mn, Zr, and Hf contents. These results can partially explain the compositional heterogeneity found in the PG materials previously reported [14].

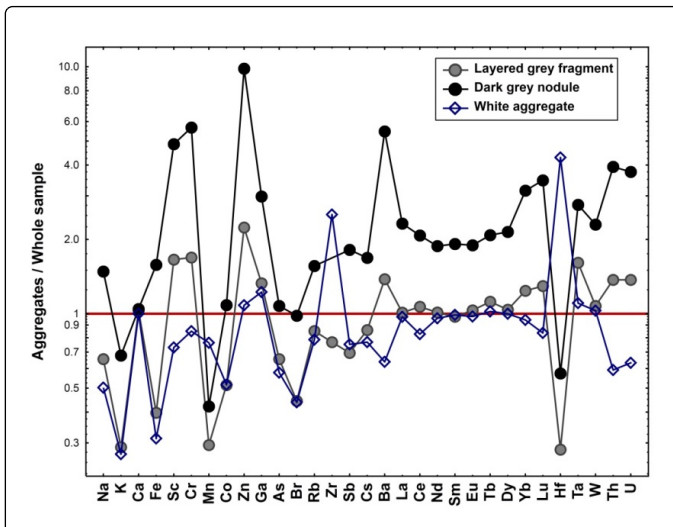


Figure 4: Chemical contents of the aggregates sample relative to the whole sample (PG #1) (Barreiro, Portugal).

Several morphologies were found in the PG particles mainly composed by Ca and S, like tabular, acicular, rhombic, and small crystal clusters (Figure 5), with different sizes in agreement with morphology found for other PG [40].

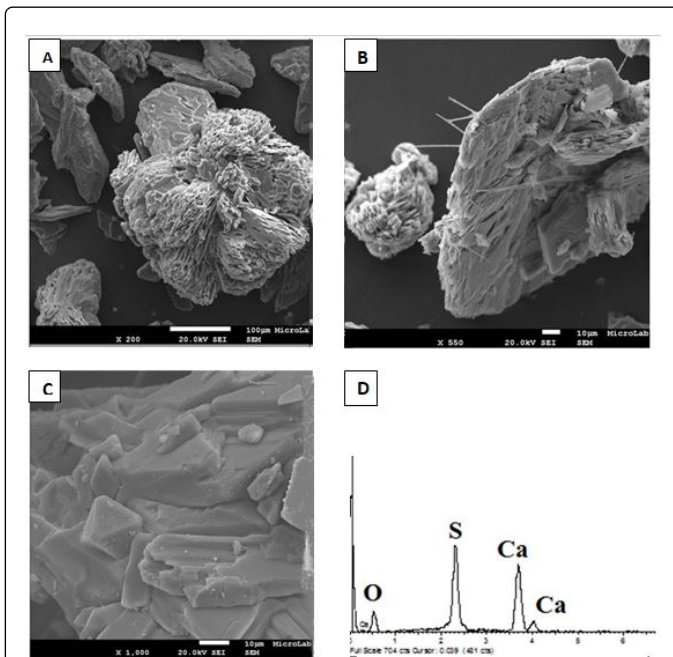


Figure 5: Morphology of PG particles of Barreiro stockpile (Portugal): a) small crystals clusters; b) acicular crystals; c) tabular and rhombic forms; and d) SEM-EDX spectrum of PG crystals.

Several slightly bright particles were found as agglomerates displaying a high degree of porosity (Figures 6 a and b). Porous particles with donut shape were in general less than 1000 nm in diameter. These particles composed of Ca, F, P, S and Al (Figure 6c), may correspond to secondary phosphates.

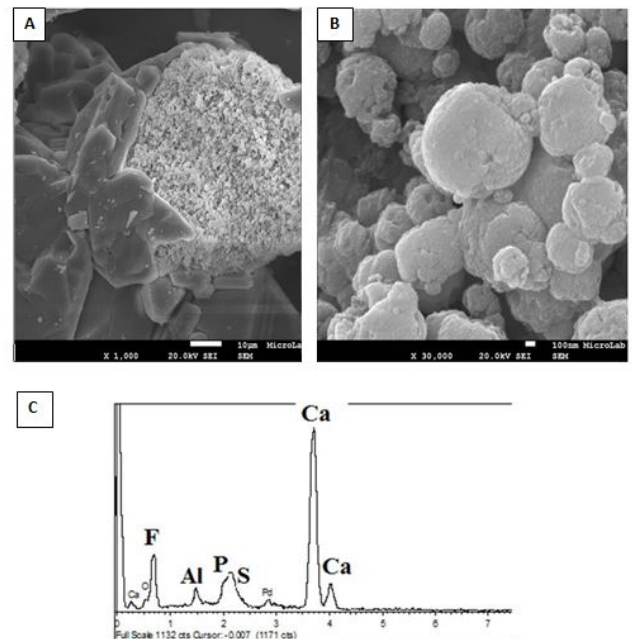


Figure 6: Morphology of particles occurring on the surface of tabular PG particles of Barreiro stockpile (Portugal): a) tabular and donut shape porous particles; b) donut shape porous particles amplified from a); and c) SEM-EDX spectrum of donuts shape particles.

The significant amount of fluorine found in these phosphate particles may be inherited from the parent rock. As already reported elsewhere [41,42], fluorine is distributed between the acid product and PG as well as in gases and vapors evolved from the acid concentration plant during processing. The presence of aluminum in minerals could indicate the aluminum phosphate which is insoluble and more often rich on ^{226}Ra [37].

Natural radioactivity

The radiometric results obtained for PG, soil and dark grey aggregates are shown in Table 3. In all the samples the majority of the radioactivity was mainly from the ^{238}U decay series. The activity concentrations in PG samples ranged from 81-184 Bq kg^{-1} for ^{238}U , from 663-802 Bq kg^{-1} for ^{226}Ra and from 681-870 Bq kg^{-1} for ^{210}Pb . These values are in close agreement with those previously reported for the same PG stockpile [11], 1043 Bq kg^{-1} for ^{226}Ra , 586 Bq kg^{-1} for ^{210}Pb and 156 Bq kg^{-1} for ^{238}U . The ^{235}U contents obtained in this work were low, with a mean value of 18 Bq kg^{-1} . The activity concentrations of ^{228}Ra , a ^{232}Th decay product, were lower than the detection limit. Concerning the ^{226}Ra activities, lower values for PG were reported for Romania (444-544 Bq kg^{-1}) [3], Syria (318 \pm 50 Bq kg^{-1}) [43], Spain (South of Huelva-278-662 Bq kg^{-1}) [44] and Greece (462 Bq kg^{-1}) [45]. On the other hand, higher ^{226}Ra activity concentrations values were reported for PG from Florida (500-1200 Bq kg^{-1}), Morocco (500-1200 Bq kg^{-1}) and Israel (500-1200 Bq kg^{-1}) [46]. The dark grey aggregates, rich in bassanite, with traces of Ti oxide, have high activities of ^{226}Ra (5385 \pm 473 Bq kg^{-1}) and ^{210}Pb (5485 \pm 2302 Bq kg^{-1}). These aggregates are also strongly enriched in ^{238}U

when compared to PG whole sample (Table 3). These results indicate that the separation of “dark aggregates” prior to any application of the PG would lead to a safer use.

Isotopes	Phosphogypsum					Soil (#4)	Dark grey aggregates
	(#1)	(#2)	(#3)	Mean	St dev.		
²³⁵ U	22.6 ± 8.9	12.5 ± 9.4	20.3 ± 9.7	18.5	5.3	2.5 ± 1.4	<153
²³⁸ U	162 ± 61	184 ± 43	81 ± 16	142	54	18.8 ± 1.7	814 ± 490
²²⁶ Ra	802 ± 45	740 ± 41	663 ± 36	735	70	45.4 ± 2.3	5385 ± 473
²¹⁰ Pb	777 ± 112	870 ± 125	681 ± 97	776	95	51.5 ± 7.9	5485 ± 2302
²²⁸ Ra	<13.5	<14.4	<12.5	-	-	11.3 ± 1.2	54 ± 16
⁴⁰ K	<64.5	93 ± 43	<61	-	-	162 ± 14	<420

Table 3: Radionuclides activity concentration ± U (k=2) in Bq kg⁻¹ (dry weight) in phosphogypsum, soil and dark grey aggregates from Barreiro (Portugal).

In order to know if the radioactive equilibrium between the radionuclides in the same radioactive series has been reached, the parent to daughter ratio was calculated. The mean ratios values of ²³⁸U/²²⁶Ra and ²³⁸U/²¹⁰Pb in PG samples were 0.19 and 0.18, respectively. In the dark grey aggregates this value was 0.15 for both ²³⁸U/²²⁶Ra and ²³⁸U/²¹⁰Pb. In all cases, these values are <1 indicating radioactive disequilibrium between ²³⁸U and its progeny. This behavior is in agreement with the expected U migration to phosphoric acid. The major amounts of ²²⁶Ra and ²¹⁰Pb that remain in the PG, may represent a potential hazard to the surrounding environment. The ²²⁶Ra/²¹⁰Pb activity ratios circa 1 in all samples corroborate the idea that these radionuclides have the same behavior during the acid treatment [29,37], not being fractionated either chemically or physically and both co-precipitating with calcium sulphate [41].

In the soil sample (#4) collected in the surrounding area of the PG stockpile, the radionuclides activity concentrations, except for ⁴⁰K, are one order of magnitude lower than for PG. The radionuclides activities recorded in soil sample are within the Portuguese and worldwide range [47]. The parent/daughter ratio in the soil is 0.41 and 0.37 for ²³⁸U/²²⁶Ra and ²³⁸U/²¹⁰Pb respectively. No radioactive equilibrium between the ²³⁸U and its progeny exists in the soil sample. The ⁴⁰K activity concentrations for PG are about 2-3 times lower when compared with the soil sample (Table 3). This finding could be justified by the technological process used for phosphoric acid production as already referred 788.

The ²³⁸U activities were determined through the daughter ²³⁴Th, presuming that ²³⁴Th was in secular equilibrium with its parent. It was demonstrated that Th can be more soluble than U in acidic environments [48], leading to a likely underestimation of the ²³⁸U activity. The ²³⁸U activities determined through ²³⁴Th (by gamma spectrometry) and through the natural U concentrations (by INAA)

were analysed using the t-test for independent samples and the Spearman correlation coefficient (rs) (STATISTICATM v.12, 2015, StatSoft®). Both methods (p-value=0.702 and rs=0.996 at 95% confidence level) point to results not significantly different and highly correlated.

Conclusions

The PG whole samples from Barreiro stockpile (Portugal) show significant variation of the chemical elements and radionuclides concentrations, probably due to the occurrence of different proportions of aggregates. Gypsum is associated mainly to brushite and bassanite. On the surface of gypsum, several porous particles with donut shape were found which correspond to secondary phosphates rich in fluorine (brushite). Among the aggregates found in the PG, the dark grey ones, rich in bassanite with traces of Ti oxide, have high amounts of most of the chemical elements studied, particularly Sc, Cr, Zn, Ga, Ba, REE, Ta, W, Th and U. The REE patterns with a significant negative Ce anomaly found in PG are certainly inherited from the parent rock (phosphate rock). The majority of the radioactivity found in the PG whole samples and in the dark grey aggregates is mainly due to the ²³⁸U decay series. The highest activities of ²²⁶Ra and ²¹⁰Pb found in the PG stockpile are certainly associated with the presence of these dark grey aggregates. The previous separation of these aggregates before any application of the PG would contribute to a safer reuse of these wastes. The results obtained in this work show how radionuclides and metals can be distributed in fine particles and can be a potential radioactive source in the Tejo estuary area.

Acknowledgements

The authors would like to thank the enterprise Baía do Tejo S.A., owner of the Barreiro Phosphogypsum (PG) stockpile, for kindly allowing sampling in its premises. The C2TN/IST authors gratefully acknowledge the Fundação para a Ciência e Tecnologia (FCT) support through the UID/Multi/04349/2013 project, and also the staff of the Portuguese Research Reactor (RPI) of CTN/IST for their assistance with the neutron irradiations.

References

- Luther SM, Dudas MJ, Rutherford PM (1993) Radioactivity and chemical characteristics of Alberta phosphogypsum. *Water Air Soil Pollut* 69: 277-290.
- Perez-Lopez R, Alvarez-Valero AM, Nieto JM (2007) Changes in mobility of toxic elements during the production of phosphoric acid in the fertilizer industry of Huelva (SW Spain) and environmental impact of phosphogypsum wastes. *J Hazard Mater* 148: 745-750.
- Calin MR, Radulescu I, Calin MA (2015) Measurement and evaluation of natural radioactivity in phosphogypsum in industrial areas from Romania. *J Radioanalytical Nuclear Chem* 304: 1303-1312.
- El Afifi EM, Hilal MA, Attallah ME, El-Reefy SA (2009) Characterization of phosphogypsum wastes associated with phosphoric acid and fertilizers production. *J Environ Radioact* 100: 407-412.
- Renteria-Villalobos M, Vioque I, Mantero J, Manjon G (2010) Radiological, chemical and morphological characterizations of phosphate rock and phosphogypsum from phosphoric acid factories in SW Spain. *J Hazard Mater* 181: 193-203.
- Caraveteanu AM, Marincea S, Dumitras DG (2009) Mineralogical and Geochemical data on the Romanian phosphogypsum. *Roman J Mineral* 84: 10-11.
- Kacimi L, Simon-Masseron A, Ghomari A, Derriche Z (2006) Reduction of clinkerization temperature by using phosphogypsum. *J Hazard Mater* 137: 129-137.

8. Dippel SK (2004) Mineralogical and geochemical characterization of phosphogypsum waste material and its potential for use as backfill at WMC fertilizers' mine site.. Masters (Research) Thesis, James Cook University, Phosphate Hill, N-W Queensland.
9. Tyler G (2004) Rare earth elements in soil and plant systems- A review. *Plant Soil* 267: 191–206.
10. Sanders LM, Luiz-Silva W, Machado W, Sanders CJ, Marotta H, et al. (2013) Rare earth element and radionuclide distribution in surface sediments along an estuarine system affected by fertilizer industry contamination. *Water Air Soil Poll* 224: 1742.
11. Carvalho FP (1995) 210Pb and 210Po in sediments and suspended matter in the Tagus estuary, Portugal. Local enhancement of natural levels by wastes from phosphate ore processing industry. *Sci Total Environ* 159: 201-214.
12. Simarsul (2006) Estudo de impacto ambiental da ETAR Barreiro/Moita. Resumo nao-tecnico. Atkins Portugal-Consultores e Prijectistas Internacionais, Lda.
13. Carvalho FP (1997) Distribution, cycling and mean residence time of 226Ra, 210Pb and 210Po in the Tagus estuary. *Sci Total Environ* 196: 151-161.
14. Carvalho FP, Oliveira JM, Silva L, Malta M (2013) Radioactivity of anthropogenic origin in the Tejo estuary and need for improved waste management and environmental monitoring. *Int J Environ Stud* 70: 952-963.
15. Corisco JAG, Mihalik J, Madruga MJ, Prudêncio MI, Marques R, et al. (2017) Natural radionuclides, rare earths and heavy metals transferred to the wild vegetation covering a phosphogypsum stockpile at Barreiro, Portugal. *Water Air Soil Poll* 228:235.
16. Brindley GW, Brown G (1980) Crystal Structures of Clay Minerals and their X-ray Identification. Mineralogical Society, London. diffraction
17. JCPDS (1993) Mineral powder diffraction file: databook: sets 1-42/ compiled by the International Centre for Diffraction Data in cooperation with the American Ceramic Society, sets 1-42, USA.
18. Govindaraju K (1994) Compilation of working values and sample description for 383 geostandards. *Geostandard Newslett* 18: 1-158.
19. Fernandes AC, Santos JP, Marques JG, Kling A, Ramos AR, et al. (2010) Validation of the Monte Carlo model supporting core conversion of the Portuguese Research Reactor (RPI) for neutron fluence rate determinations. *Ann Nucl Energy* 37: 1139-1145.
20. Gouveia MA, Prudêncio MI, Morgado I, Cabral JMP (1992) New data on the GSJ reference rocks JB-1a and JG-1a by instrumental neutron activation analysis. *J Radioanal Nucl Chem* 158: 115-120.
21. Prudencio MI, Valente T, Marques R, Sequeira-Braga MA, Pamplona J (2015) Geochemistry of rare earth elements in a passive treatment system built for acid mine drainage remediation. *Chemosphere* 138: 691–700.
22. Marques R, Prudencio MI, Dias MI, Rocha F (2011) Patterns of rare earth and other trace elements in different size fractions of clays of Campanian-Maastrichtian deposits from the Portuguese western margin (Aveiro and Taveiro Formations). *Chem Erde-Geochem* 71: 337-347.
23. Marques R, Waerenborgh JC, Prudencio MI, Dias MI, Rocha F, et al. (2014) Iron speciation in volcanic topsoils from Fogo island (Cape Verde) –Iron oxide nanoparticles and trace elements concentrations. *Catena* 113: 95–106.
24. Genie™ 2000 (2004) Spectroscopy software-customization tools manual. Canberra Industries.
25. Sima O, Arnold D, Dovieta C (2001) GESPECOR-A versatile tool in gamma-ray spectrometry. *J Radioanal Nucl Chem* 249: 359-364.
26. Meresova J, Watjen U, Altitzoglou T (2012) Determination of natural and anthropogenic radionuclides in soil—results of an European Union comparison. *Appl Radiat Isot* 70: 1836–1842.
27. Pinto AJ, Carneiro J, Katsikopoulos D, Jimenez A, Prieto M (2012) The link between brushite and gypsum: miscibility, dehydration, and crystallochemical behavior in the CaHPO₄. 2H₂O-CaSO₄.2H₂O system. *Cryst Growth Des* 12: 445- 455.
28. Hurst FJ, Arnold WD (1980) Uranium control in phosphogypsum. DP Borris, PW Boody (Eds.), Proceedings of the International Symposium on phosphogypsum. Florida Institute of Phosphate Research, Lake Buena Vista, Florida 424-441.
29. Hull CD, Burnett WC (1996) Radiochemistry of Florida Phosphogypsum. *J Environ Radioact* 32: 213-238.
30. Bowen HJM (1979) Environmental chemistry of the elements. Academic Press Inc., London.
31. Marques R, Dias MI, Prudencio MI, Rocha F (2011) Upper cretaceous clayey levels from western Portugal (Aveiro and Taveiro regions): clay mineral and trace-element distribution. *Clays Clay Miner* 59: 315–327.
32. Prudêncio MI, Dias MI, Ruiz F, Waerenborgh JC, Duplay J, et al. (2010) Soils in the semi-arid area of the El Melah Lagoon (NE Tunisia)– Variability associated with a closing evolution. *Catena* 80: 9-22.
33. Anders E, Grevesse N (1989) Abundances of the elements: meteoritic and solar. *Geochim Cosmochim Acta* 53: 197-214.
34. Korotev RL (1996a) A self-consistent compilation of elemental concentration data for 93 geochemical reference samples. *Geostand Newslett* 20: 217-245.
35. Korotev RL (1996b) On the relationship between the Apollo 16 ancient regolith breccias and feldspathic fragmental breccias, and the composition of the prebasin crust in the Central Highlands of the Moon. *Meteorit Planet Sci* 31: 403-412.
36. Ramos SJ, Dinali GS, de Carvalho TS, Chaves LC, Siqueira JO, et al. (2016) Rare earth elements in raw materials and products of the phosphate fertilizer industry in South America: Content, signature, and crystalline phases. *J Geochem Explor* 168: 177-186.
37. Santos AJG, Mazilli BP, Favors DIT, Silva PSC (2006) Partitioning of radionuclides and trace elements in phosphogypsum and its source materials based on sequential extraction methods. *J Environ Radioact* 87: 52-61.
38. Prudêncio MI, Gouveia MA, Sequeira-Braga MA (1995) REE distribution in present-day and ancient surface environments of basaltic rocks (central Portugal). *Clay Miner* 30: 239-248.
39. Prudêncio MI, Dias MI, Waerenborgh JC, Ruiz F, Trindade MJ, et al. (2011) Rare earth and other trace and major elemental distribution in a pedogenic calcrete profile (Slimene, NE Tunisia). *Catena* 87: 147–156.
40. Zielinski RA, Al-Hwaiti MS, Budahn JR, Ranville JF (2011) Radionuclides, trace elements, and radium residence in phosphogypsum of Jordan. *Environ Geochem Health* 33: 149-165.
41. Beddow H, Black S, Read D (2006) Naturally occurring radioactive material (NORM) from a former phosphoric acid processing plant. *J Environ Radioact* 86: 289-312.
42. Schroder K (1998) Phosphoric acid and phosphates, Wiley-VCH.
43. Al Attar L, Al-Oudat M, Kanakri S, Budeir Y, Khalily H, et al. (2011) Radiological impacts of phosphogypsum. *J Environ Manage* 92: 2151-2158.
44. Martinez-Sanchez MJ, Perez-Sirvent C, Garcia-Lorenzo ML, Martinez-Lopez S, Bech J, et al. (2014) Use of bioassays for the assessment of areas affected by phosphate industry wastes. *J Geochem Explor* 147: 130-138.
45. Papageorgiou F, Godelitsas A, Mertzimekis TJ, Xanthos S, Voulgaris N, et al. (2016) Environmental impact of phosphogypsum stockpile in remediated Schistos waste site (Piraeus, Greece) using a combination of γ-ray spectrometry with geographic information systems. *Environ Monit Assess* 188:133.
46. Cioroianu TM, Bunus F, Filip D, Filip Gh (2001) Environmental considerations on uranium and radium from phosphate fertilizers. IAEA-TECDOC, 1244, International Atomic Energy Agency, Vienna 215-224.
47. UNSCEAR (2008) Sources and effects of ionizing radiation. United Nations Scientific Committee on the Effects of Atomic Radiation, United Nations Publication, New York, USA 1.
48. Ahmed H, Young S, Shaw G (2012) Solubility and mobility of thorium and uranium in soils: The effect of soil properties on Th and U concentrations in soil solution. In: Proceedings of EGU General Assembly Conference, 22-27 April, 2012, Vienna, Austria, Geophysical Research Abstracts 14: 2994.